Introduction to biomolecular NMR spectroscopy

Part I

Michael Sattler, EMBL Heidelberg
www.EMBL-Heidelberg.de/nmr/sattler

- History
- Applications of NMR
- Principles of Nuclear Magnetic Resonance
- NMR observables and parameters for structure determination
- Literature

Development of nuclear magnetic resonance

History

1946	Bloch, Purcell	first nuclear magnetic resonance
1955	Solomon	NOE (nuclear Overhauser effect)
1966	Ernst, Anderson	Fourier transform NMR
1975	Jeener, Ernst	2D NMR
1985	Wüthrich	first solution structure of a small protein (BPTI) from NOE based distance restraints

→ NMR is about 25 years younger than X-ray crystallography

1987/8	3D NMR + ^{13}C, ^{15}N isotope labeling
1996/7	new long range structural parameters:
	- projection angles from: residual dipolar couplings (partial alignment)
	T_1/T_2 relaxation time ratio (anisotropic diffusion)
	- projection angles (cross-correlated relaxation)
	- TROSY (molecular weight > 100 kD)

Nobel prizes

1944	Physics	Rabi (Columbia)
1952	Physics	Bloch (Stanford), Purcell (Harvard)
1991	Chemistry	Ernst (ETH)

Applications of nuclear magnetic resonance

Solid state NMR

→ usually very large line-widths due to large dipolar couplings (kHz)

Chemical analysis

Polymers

Membrane peptides and proteins

Liquid state, high-resolution NMR

→ usually narrow line-widths depending on molecular weight and tumbling rate in solution

Chemical analysis

Metabolic pathways

Constitution, conformation and dynamics of small molecules

Biomolecular NMR: structural biology

Magnetic Resonance Imaging (MRI)

Magnetic Resonance Imaging (MRI)

- **Imaging: *in vivo* studies on humans**
- **Tomography: cancer diagnostics**
- **Localized spectroscopy: study metabolism *in vivo***

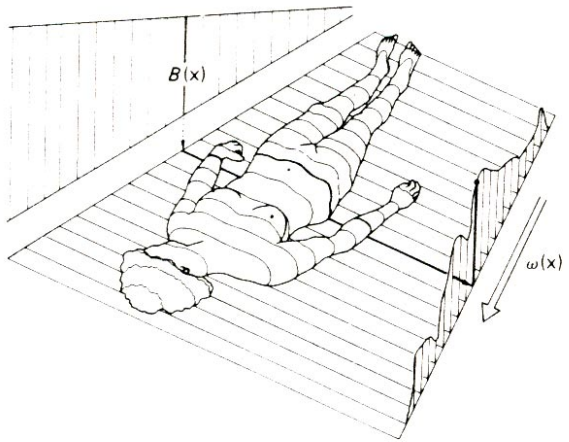

FIG. 10.0.2. Basic idea of NMR imaging: the NMR signal is recorded in the presence of a linear magnetic field gradient $B(x)$, such that the resonance frequency $\omega(x)$ is a linear function of the spatial coordinate.

(Ernst et al, "Principles of Nuclear Magnetic Resonance")

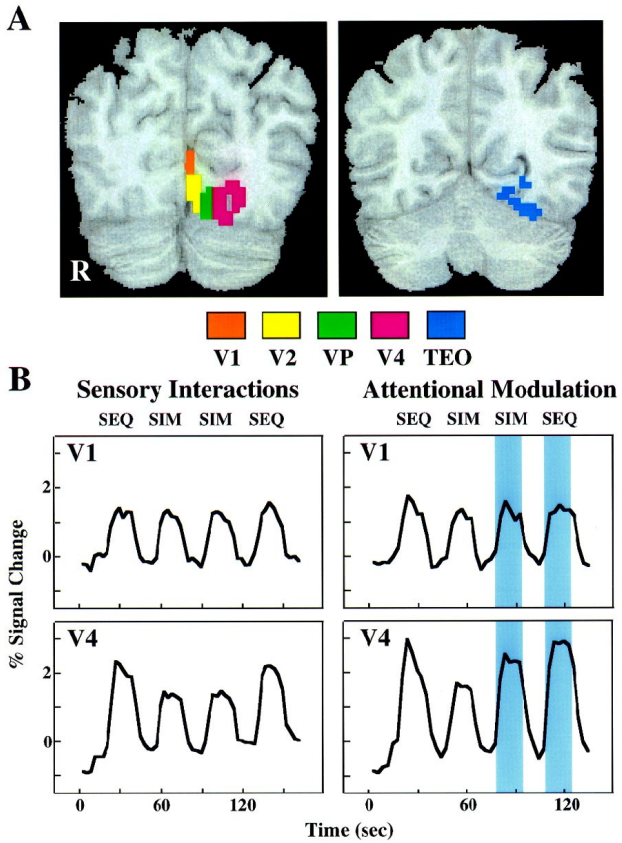

Mechanisms of Directed Attention in the Human Extrastriate Cortex as Revealed by Functional MRI

Sabine Kastner, Peter De Weerd, Robert Desimone, and Leslie G. Ungerleider, Science 1998 October 2; 282: 108-111.

Structure determination of biomolecules by NMR

- why NMR?
- solution vs. crystal → no crystal needed, native conditions?
- nucleic acids: difficult to crystallize, affected by crystal packing
- potential to study dynamics, conformational averaging, chemical reactions, folding
- study dynamics in picosecond to seconds time scales
- ligand binding in solution for large molecular assemblies
- NMR detects protons, X-ray heteroatoms ("histidine problem")
- structural quality: precision and accuracy
- molecular weight: X-ray: >200 kDa, NMR < 50 kDa
- => NMR and X-ray crystallography are complementary

PDB entries 07-May-2002

	Proteins	Protein/DNA Protein/RNA	DNA/ RNA	Carbo- hydrates
X-ray	13580	649	610	14
NMR	2236	84	443	4

Principles of NMR: nuclear spin

A nuclear spin of $I > 0$ is associated with a nuclear magnetic dipole moment $\mu = \gamma I$

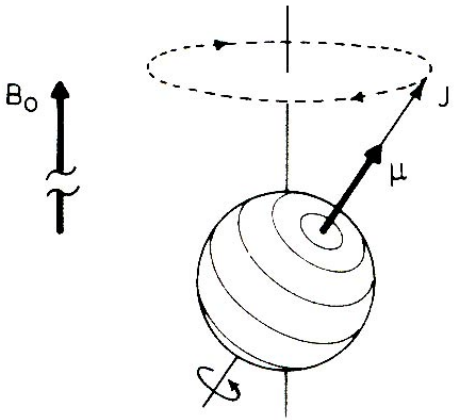

precession

$E = \mu B_0$

TABLE 1.1
Properties of Selected Nuclei[a]

Nucleus	I	γ (T · s)$^{-1}$	γ_{rel}(T s)$^{-1}$	Natural abundance (%)
^{1}H	$\frac{1}{2}$	2.6752×10^{8}	**1.0**	99.98
^{2}H	1	4.107×10^{7}	**0.15**	0.02
^{13}C	$\frac{1}{2}$	6.728×10^{7}	**0.25**	1.11
^{14}N	1	1.934×10^{7}		99.64
^{15}N	$\frac{1}{2}$	-2.712×10^{7}	**0.1**	0.36
^{17}O	$\frac{5}{2}$	-3.628×10^{7}		0.04
^{19}F	$\frac{1}{2}$	2.5181×10^{8}		100.00
^{23}Na	$\frac{3}{2}$	7.080×10^{7}		100.00
^{31}P	$\frac{1}{2}$	1.0841×10^{8}	**0.41**	100.00
^{113}Cd	$\frac{1}{2}$	5.934×10^{7}		12.26

[a] The angular momentum quantum number, I, and the gyromagnetic ratio, γ, and natural isotopic abundance for nuclei of particular importance in biological NMR spectroscopy are shown.

(Cavanagh, et al. “Protein NMR spectroscopy”)

Principles of NMR: energy levels & populations

Energy of a spin in a magnetic field:

$E = \mu B_0 = \gamma I B_0$

$I = \pm \frac{1}{2} \hbar$ nuclear spin

μ = magnetic moment

γ = gyromagnetic ratio

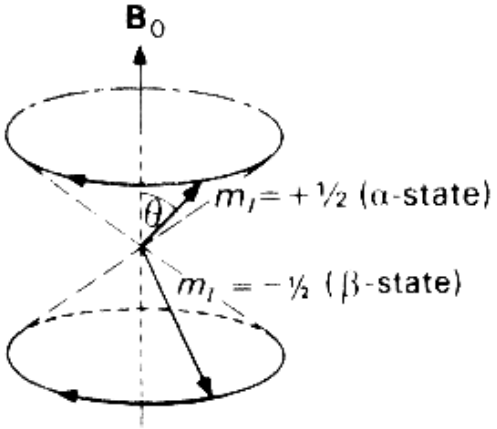

Fig. 1-5 The two precessional cones for a spin-$\frac{1}{2}$ nucleus in a magnetic field, showing typical spin vectors. The angle θ is 54° 44′ in this case.

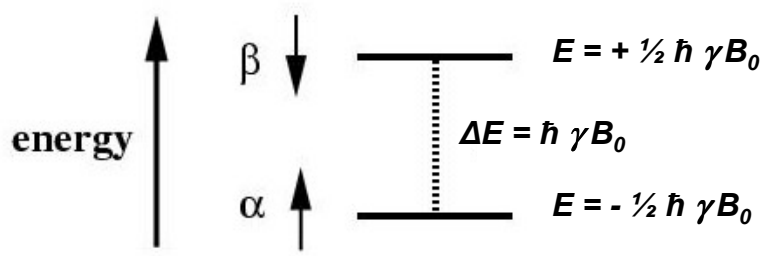

Boltzmann distribution: $\frac{N(\alpha)}{N(\beta)} = e^{\frac{2\mu B_0}{kT}} \sim 1 + \frac{2\mu B_0}{kT} = \frac{1.00001}{1}$

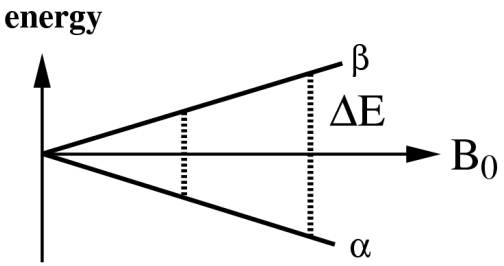

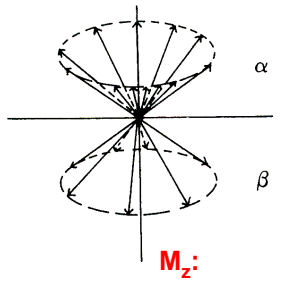

M_z: z-magnetization

- In an ensemble of spin ½ nuclei the α (up) and β (down) energy levels are populated according to Boltzmann statistics.
- This leads to a small effective magnetization along the *z*-axis (B_0).
- No *x*- or *y*-magnetization is observed since the spin vectors are not *phase coherent*, i.e. they precess independent from each other around B_0 and their x,y components thus average to zero.

Principles of NMR: sensitivity of NMR spectroscopy

$$S/N \sim N\ \gamma_{exc}\ \gamma_{det}^{3/2}\ B_0^{3/2}\ NS\ T_2^{1/2}$$

S/N	signal-to-noise	
N	number of spins	→ sample concentration
γ_{exc}	gyromagnetic ratio of excited spins	
γ_{det}	gyromagnetic ratio of detected spins	
B_0	static magnetic field	
	(e.g. 14.1 Tesla or 600 MHz for ^1H)	
NS	number of scans	→ experimental time
T_2	transverse relaxation time	→ line width $\Delta\nu \sim 1/(\pi T_2)$

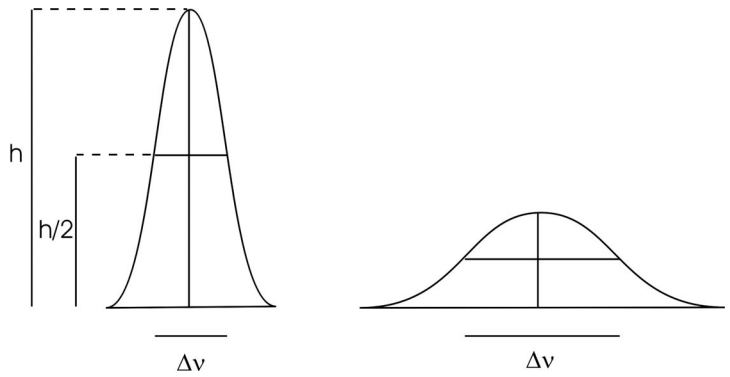

Slow relaxation Fast relaxation

The electromagnetic spectrum

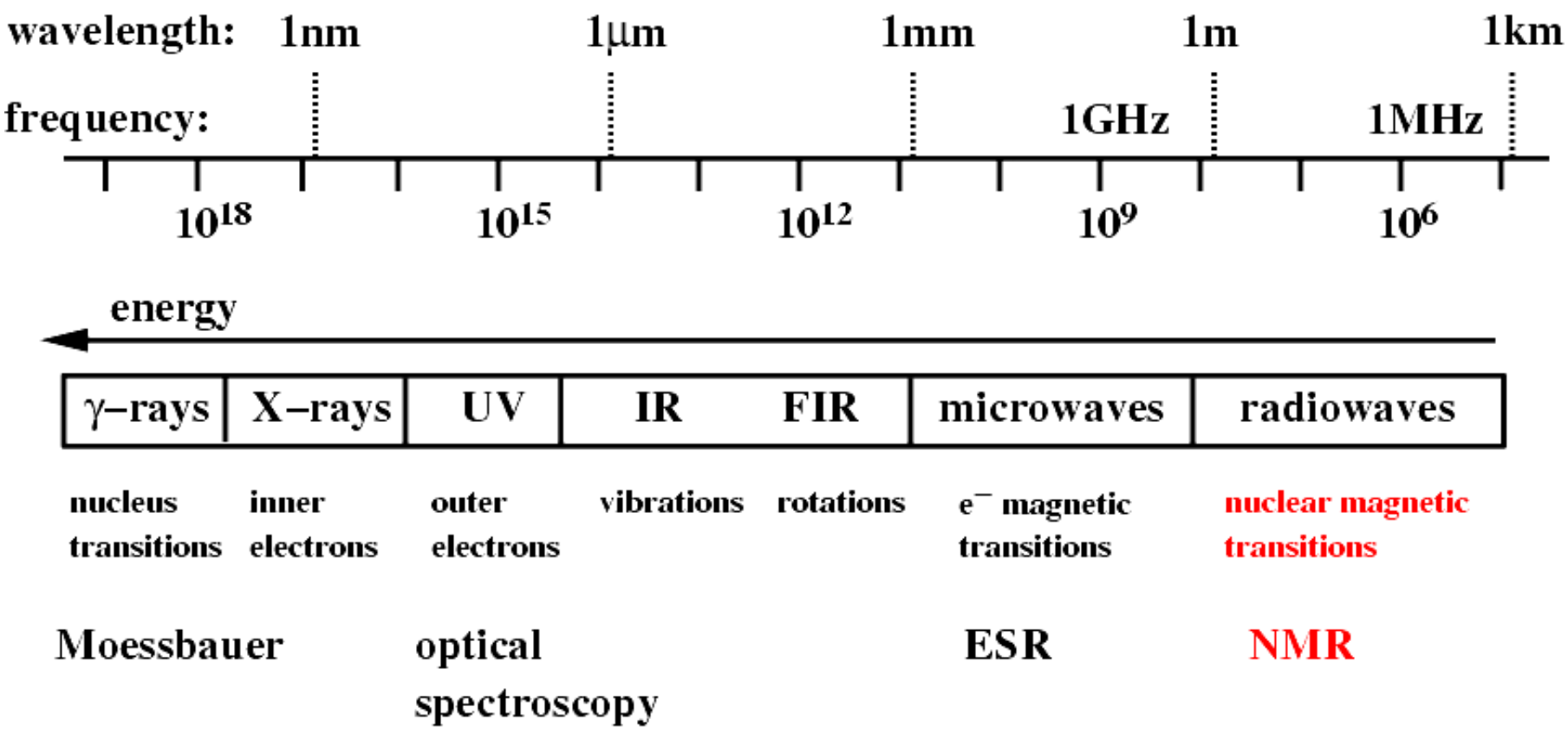

Principles of NMR: Fourier transform NMR

CW

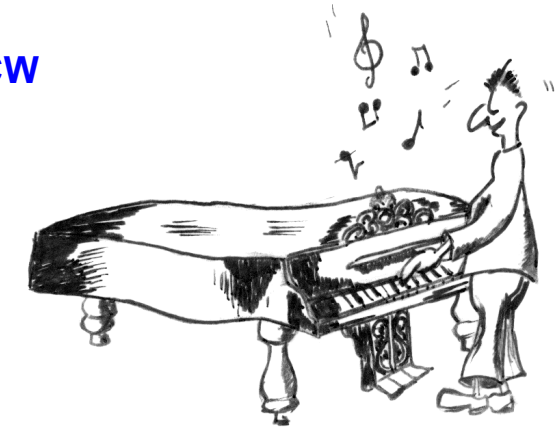

FT

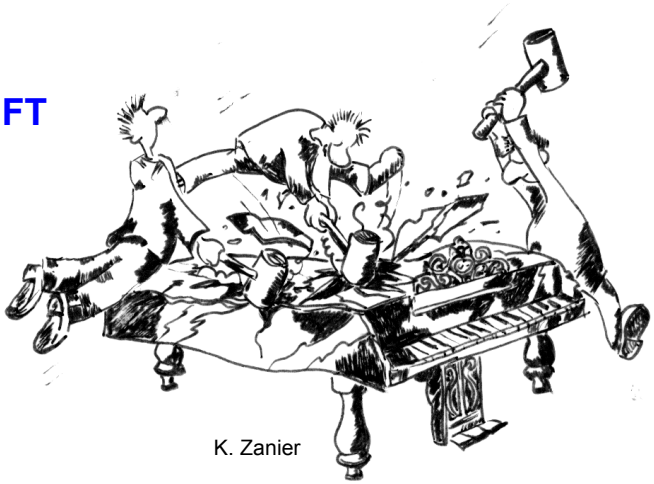

K. Zanier

$$f(t) \underset{IFT}{\overset{FT}{\rightleftharpoons}} F(\omega)$$

time domain | frequency domain

Continuous Wave (CW) NMR

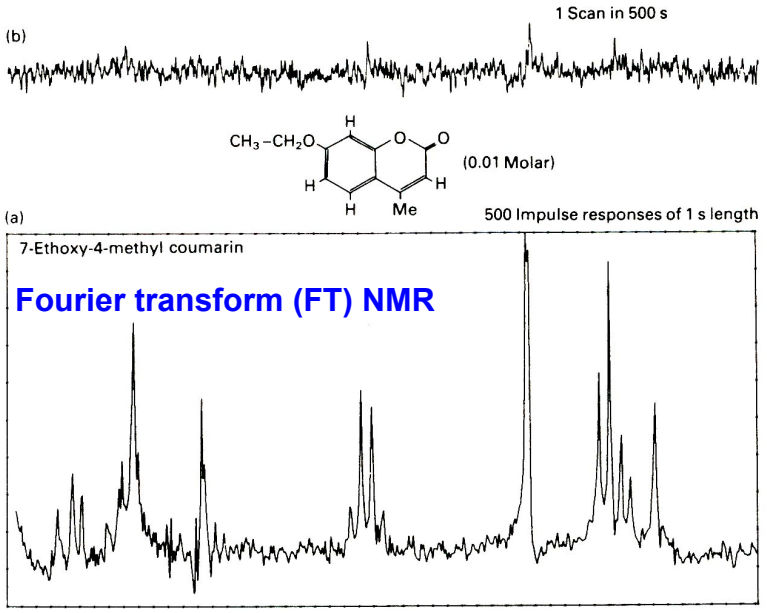

(Ernst, et al. “Principles of Nuclear Magnetic Resonance”)

NMR spectrometer hardware

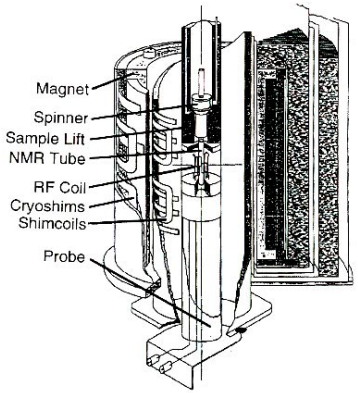

FIGURE 3.2 Cutaway diagram of a superconducting magnet. The probe, sample spinner, and room-temperature shim coils are positioned coaxially in the room-temperature bore of the magnet. The solenoid and cryoshim coils are immersed in liquid helium. The helium dewar is surrounded by a radiation shield and a liquid nitrogen dewar. Diagram courtesy of Bruker Instruments, Inc.

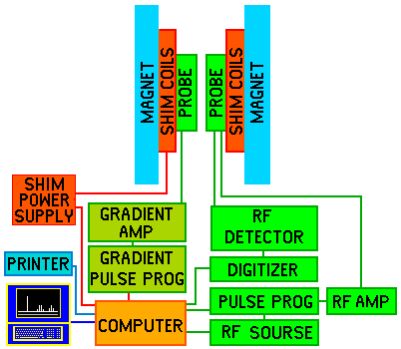

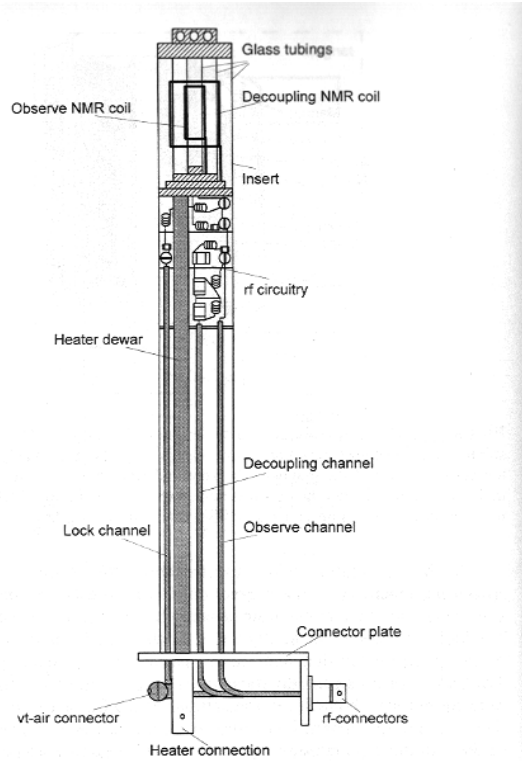

FIGURE 3.3 Probe assembly. Major components of a high-resolution NMR spectroscopy rf probe are illustrated. Diagram courtesy of Bruker Instruments, Inc.

(Cavanagh, et al. “Protein NMR spectroscopy”)

magnet (B_0)

spectrometer

probe
(rf + receiver coil)

1-dimensional NMR spectroscopy

A radio frequency (rf) pulse along x causes the z-magnetization (M) to precess around the x-axis. The pulse is switched off after a 90° rotation leaving the magnetization along the y-axis.

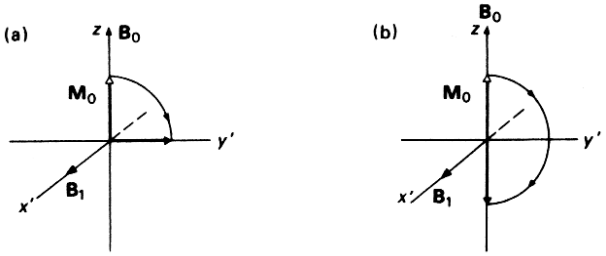

90°(x) pulse 180°(x) pulse

→ **In this state, the spin vectors whose population difference gave rise to the z-magnetization before the rf pulse have become phase coherent, e.g. are oriented towards the y-axis.**

→ **The α- and β-states are equally populated, thus no z-magnetization is left.**

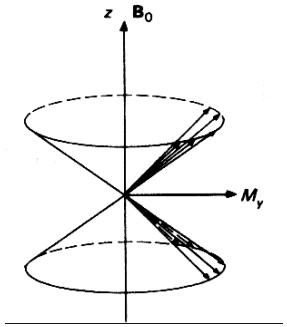

M_y: y-magnetization

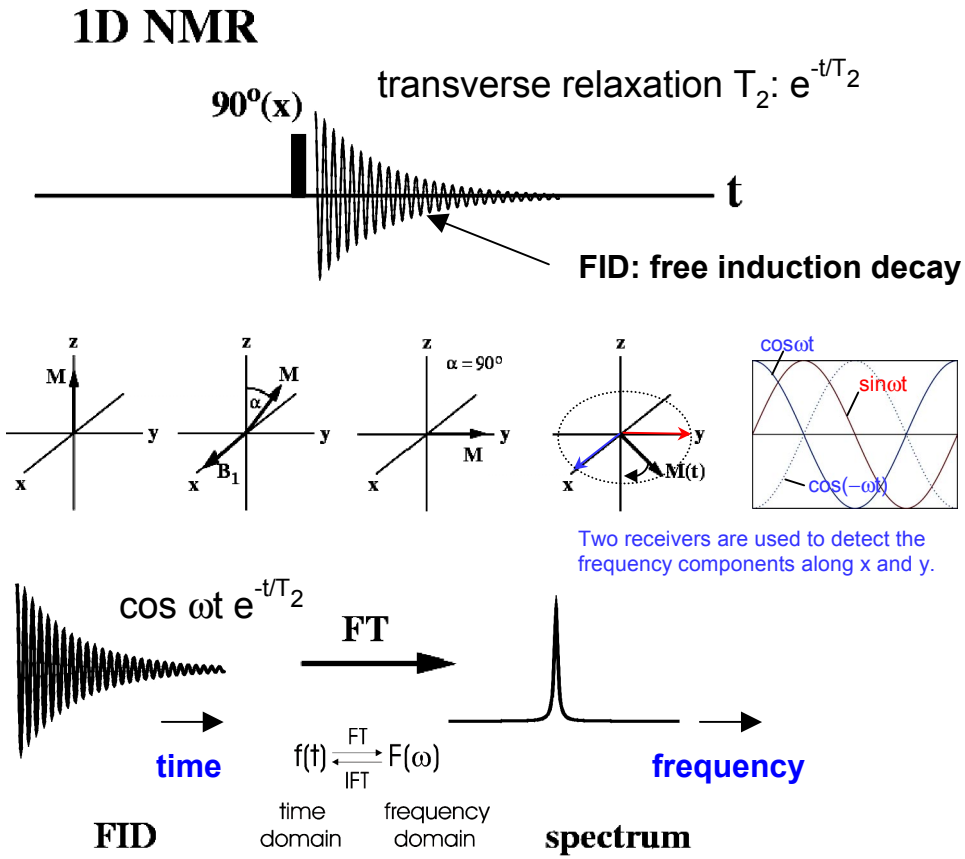

$90^o(x) = 90^o$ rf pulse along x–axis

FT = Fourier transformation F(t) –> F(ω)

FID = free induction decay

Relaxation

After the rf pulse, the Boltzmann equilibrium is restored by relaxation. This is a result of interactions of the spins with each other and with the environment (the "lattice").

→ The equilibrium z-magnetization, M_0, is restored by longitudinal or spin-lattice relaxation which is described by a relaxation time constant T_1.

$$M_z(t) - M_0 = [M_z(0) - M_0] \exp(-t/T_1)$$

T_1 is measured by inverting the equilibrium z-magnetization $M_z(t) = -M_z$, and measuring the recreation of $+M_z$ magnetization in *inversion recovery* experiments (180^o–τ – 90^oFID).

→ The decay of x,y magnetization reflects the loss of phase coherence of the spin vectors in the x,y plane and is called transverse or spin-spin relaxation described by a relaxation time constant T_2.

$$M_y(t) = M_y(0) \exp(-t/T_2)$$

T_2 is measured as the decay of transverse (x- or y-magnetization), for example using a spin-echo sequence (90^o–τ – 180^o–τ FID) with a variable delay τ.

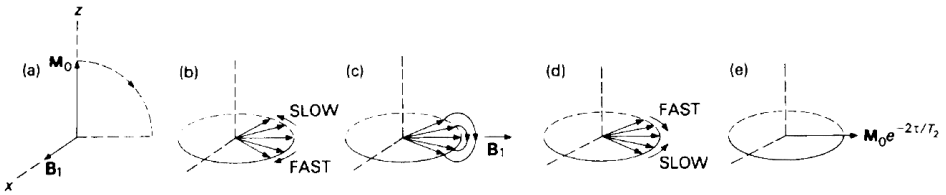

Fig. 3-14 The spin-echo effect (a) a 90°_x pulse puts M_0 into the y' direction, (b) the spin isochromats[11] fan out, (c) a 180°_x pulse interchanges slow and fast spins at time τ, (d) refocusing occurs, (e) the echo at time 2τ.

Hahn spin-echo experiment

(Harris "Nuclear Magnetic Resonance Spectroscopy")

T_1 and T_2 depend on the correlation time τ_c for random molecular tumbling (thus, on the molecular weight) and also on the B0 magnetic field strength:

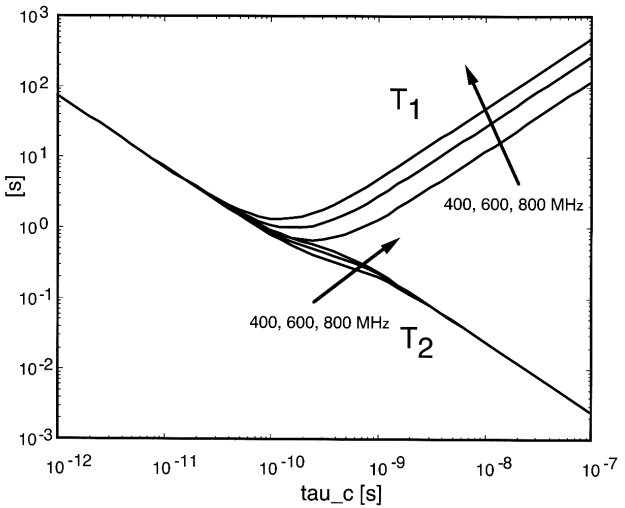

molecular weight →

Chemical shifts

- At the local position of a nuclear spin within a molecule the external magnetic field B_0 is shielded by the local electronic environment. The external field is therefore scaled (σ = shielding constant) : $B = B_0 (1-\sigma)$.
- As a result, for example, the H^N and Hα protons in the peptide backbone of a protein have different chemical shift regions which helps to identify them.
- Chemical shifts are normalized with respect to the static magnetic field and expressed as ppm.

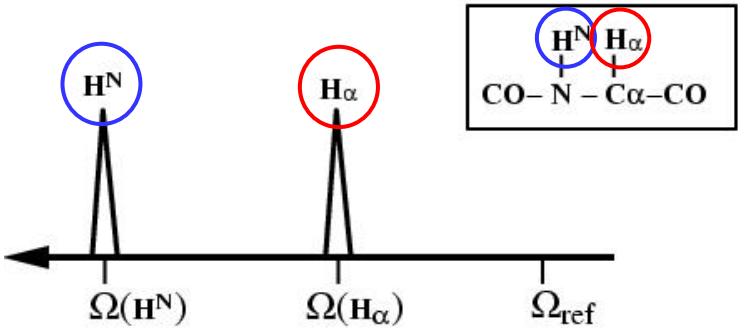

$$\delta(\text{ppm}) = (\Omega - \Omega_{ref})/\omega_0 * 10^6$$

chemical shifts in parts per million [ppm] are *independent* of the field strenght of the static magnetic B_0 field

(Cavanagh, et al. "Protein NMR spectroscopy")

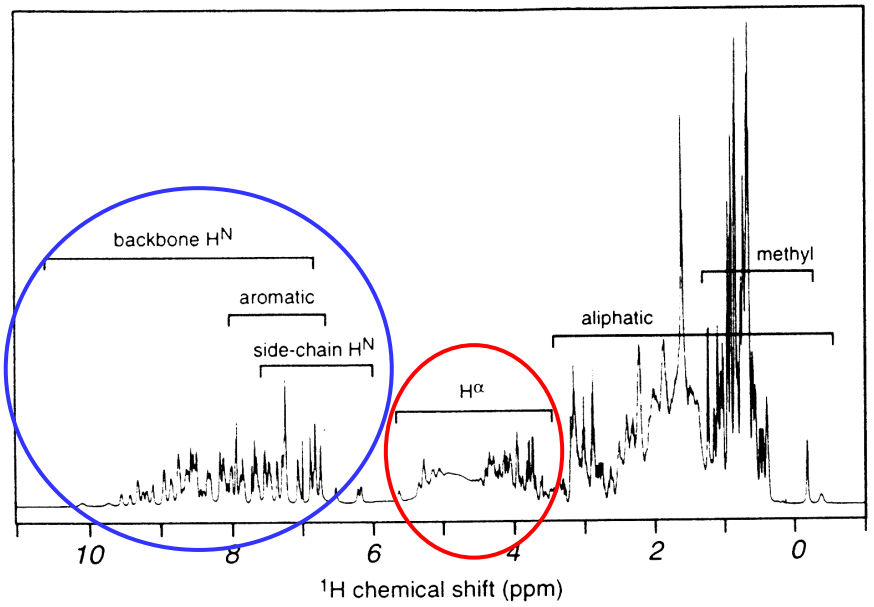

Scalar/J-coupling

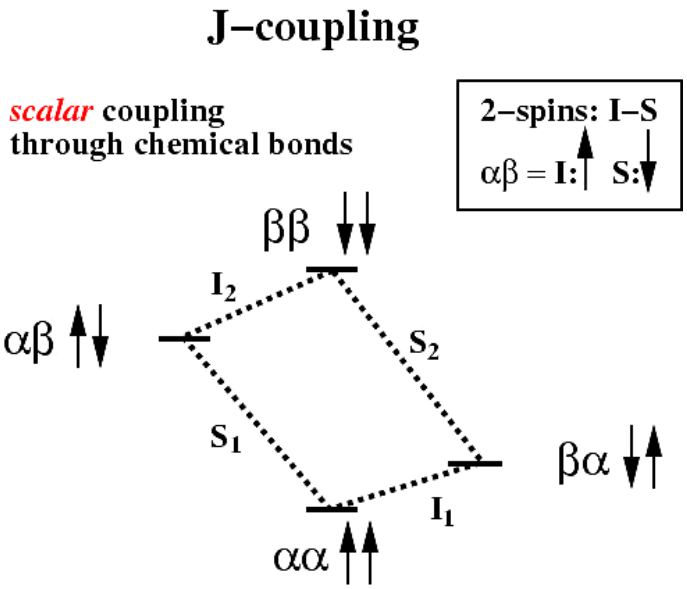

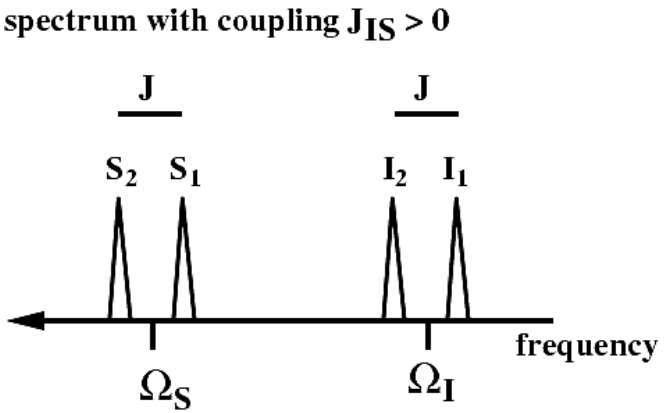

Sign of J-coupling

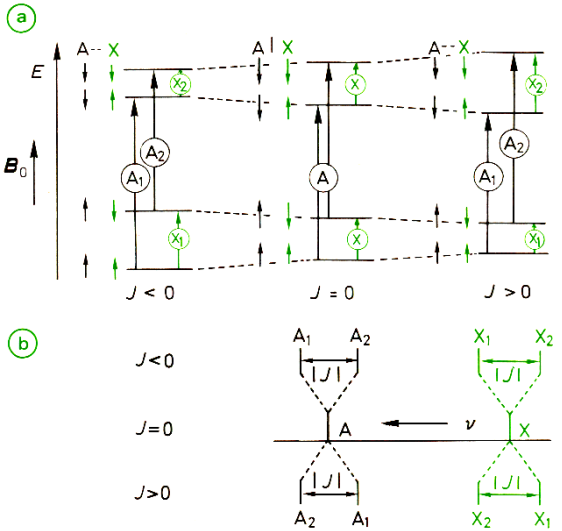

Abb. 3.3 **a** Die vier möglichen Spin-Einstellungen und Energieniveaus eines Zwei-Spin-Systems ($m = \pm 1/2$) und die zugehörigen Kernresonanz-Übergänge bei $J \lessgtr 0$: ↑ A-Resonanzen, ↑ X-Resonanzen
b Strichspektren der Kopplungsfälle $J < 0$, $J = 0$, $J > 0$

Multiplicities

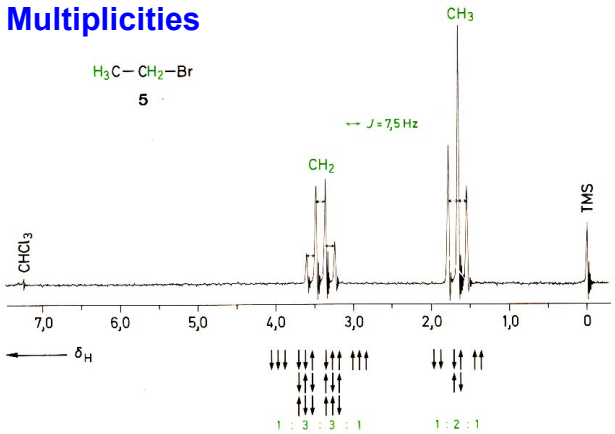

Scalar/J-coupling: Karplus curve

J-couplings across 3 bonds depend on the intervening central torsion angle.

The 3-bond H^N,Hα coupling $^3J(H^N,H\alpha)$ is a measure of the backbone torsion angle ϕ.

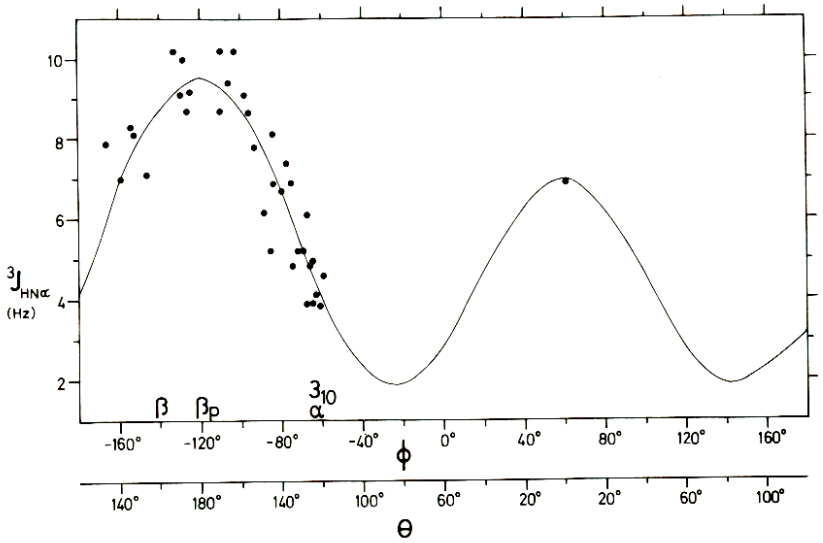

Figure 9.2. Plot of $^3J_{HN\alpha}$ versus the torsion angle $\theta = |\phi - 60°|$ in BPTI. ϕ was obtained from the crystal structure and $^3J_{HN\alpha}$ from solution studies. The filled circles represent individual amino acid residues. The curve corresponds to the best fit obtained with Eq. (9.1). ϕ values for regular secondary structures are indicated by α, 3_{10}, β, and β_p (from Pardi et al., 1984).

(Wüthrich "NMR of proteins and nucleic acids")

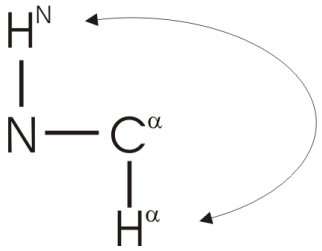

$^3J(H^N,H\alpha)$ = 4-10 Hz

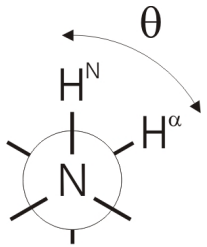

$\phi = \theta - 60^0$

2D NMR: COSY

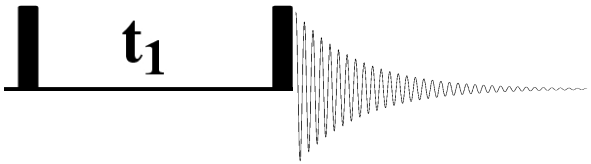

a)

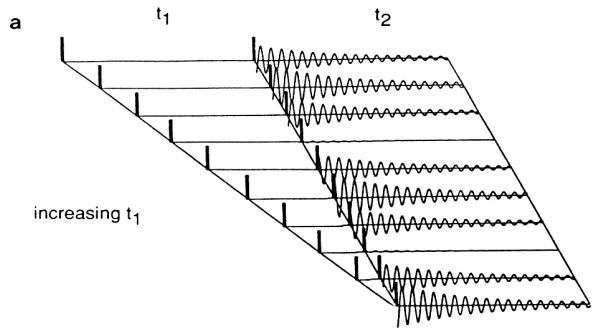

b)

Fourier transformation

with respect to t_2

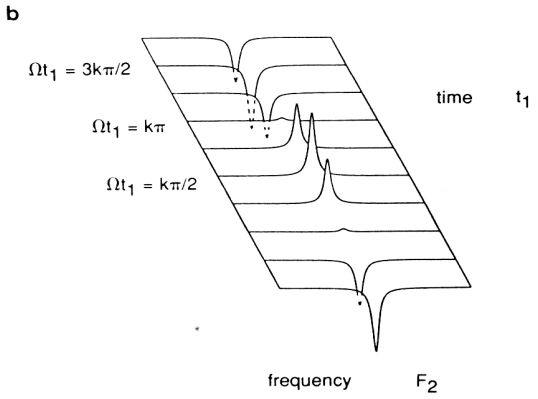

c) 2D FT

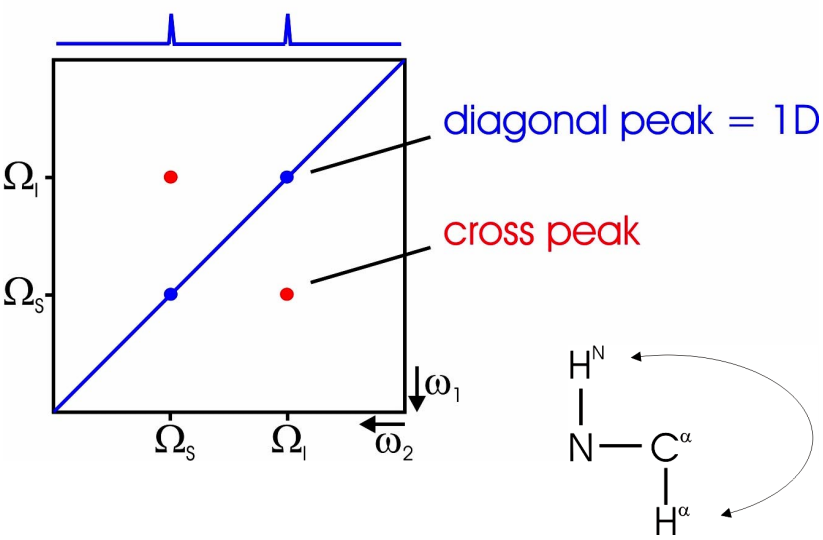

Cross peaks contain new information as a result of magnetization transfer during the 2D experiment.

In a COSY spectrum the scalar J-coupling yields transfer of magnetization from the H^N to the Hα and vice versa which belong to the same scalar couplied spin system.

The cross peak therefore provides information about intraresidue $^1H,^1H$ correlations.

2D NMR: COSY

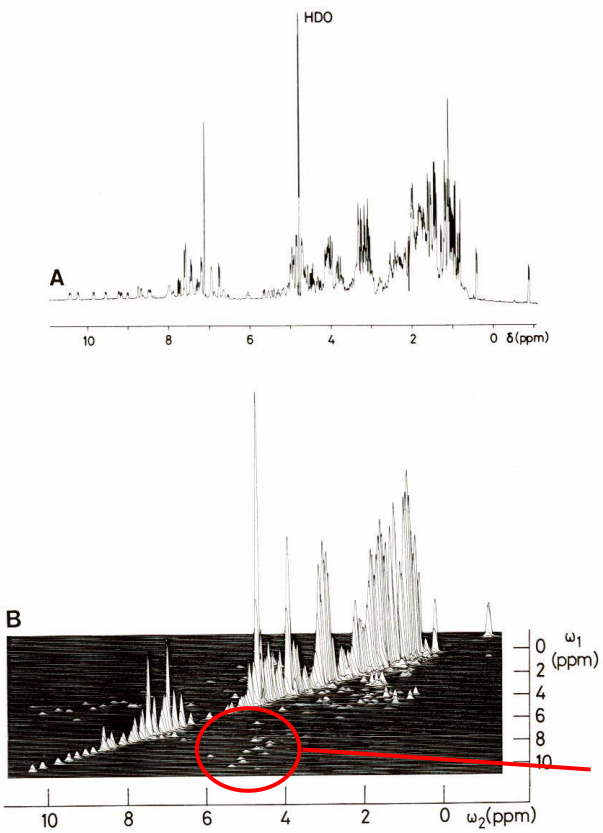

Figure 5.8. ^{1}H COSY of a freshly prepared D_2O solution of inhibitor *K* (0.01 *M*, pD 3.4, 25°C; 360 MHz; absolute value). *(A)* 1D ^{1}H NMR. *(B)* Stacked plot of COSY spectrum. *(C)* Contour plot of COSY spectrum. Above the diagonal, broken and dotted lines indicate how connectivities between distinct diagonal peaks are established via the cross peaks. Below the diagonal, solid lines define the regions a–h, which contain cross peaks between distinct proton types (see text). The arrows are explained in the text.

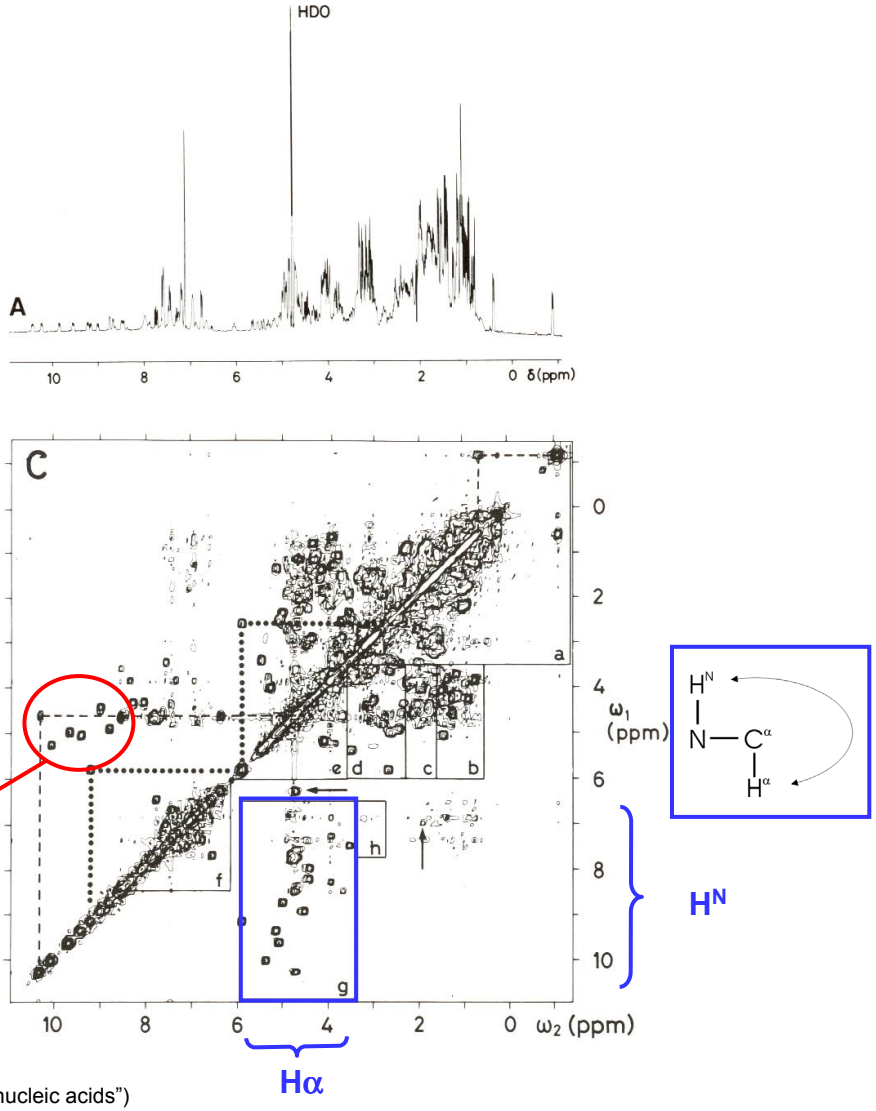

(Wüthrich “NMR of proteins and nucleic acids”)

Heteronuclear 2D NMR: H,N correlations

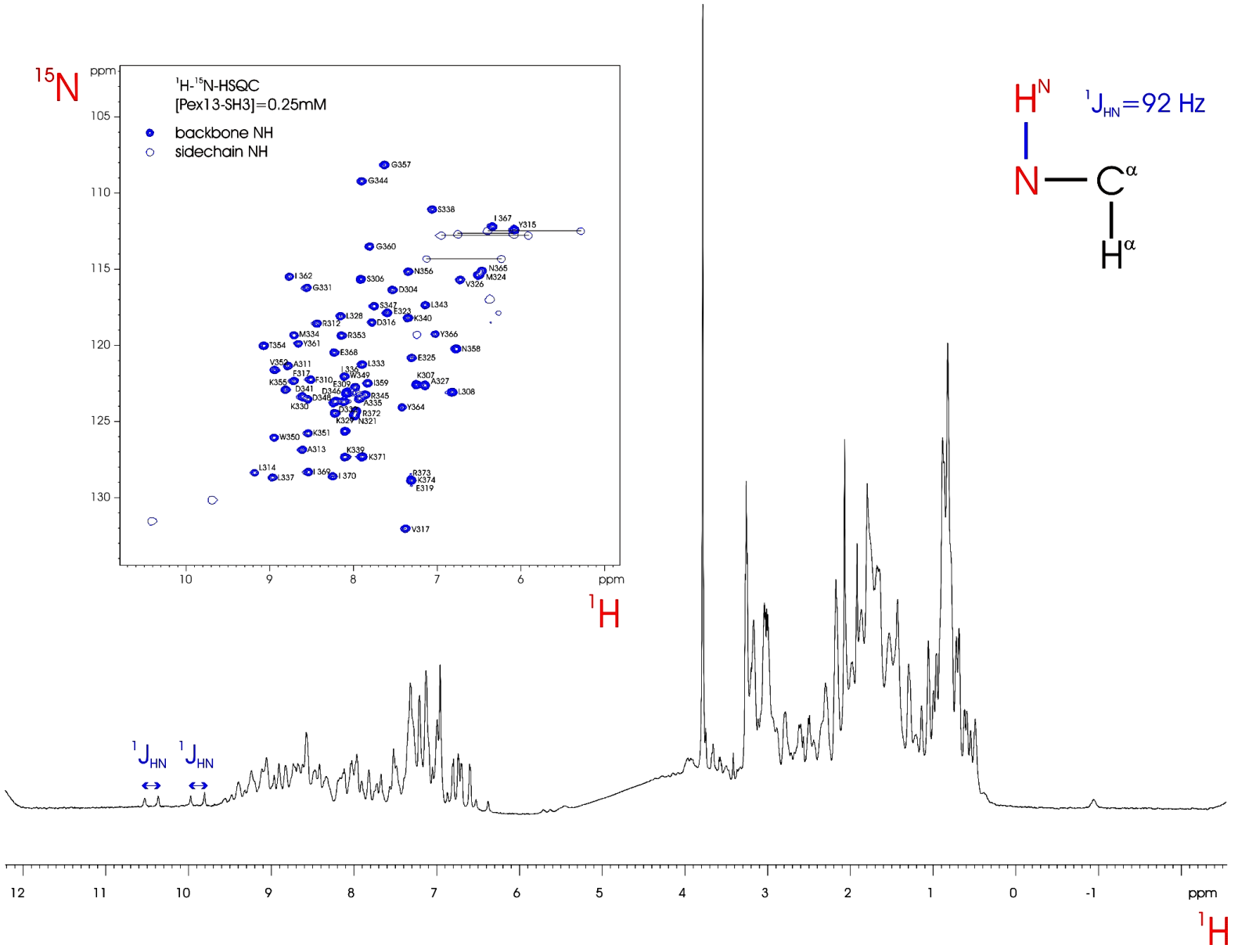

Nuclear Overhauser Effect (NOE)

NOE

I $\overset{\text{dipolar coupling}}{\underset{\text{distance } r}{\cdots\cdots}}$ **S**

dipolar **coupling through space**
–> splitting (in solid phase)
–> relaxation (in liquid phase)

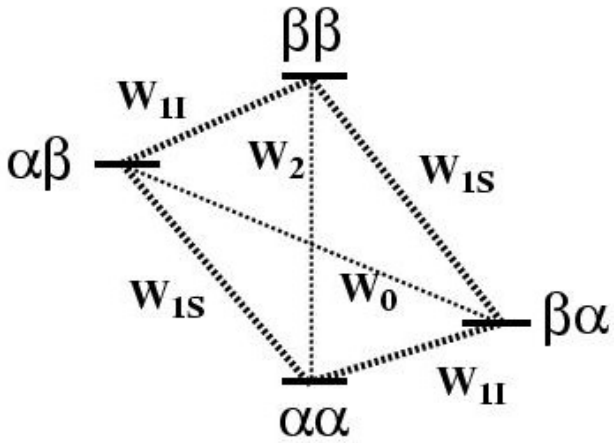

W = transition rates

The NOE is a result of spin-spin cross relaxation via W_2 and W_0 transition rates between two spins I and S.
The NOE is inverse proportional to the distance between the two interacting spin.

NOE intensity ~ $1/r^6$

This distance dependence of the NOE is used to derive proton/proton distance restraints for the structure determination by NMR.

Exchange, conformational dynamics

NMR time scale

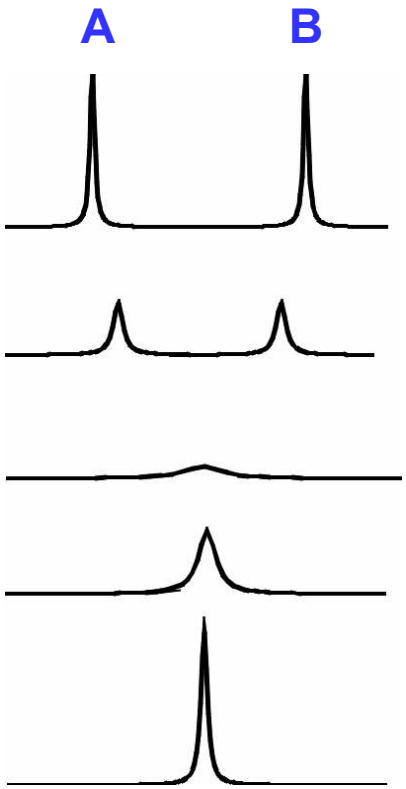

slow exchange
$k << \Delta\nu$

coalescence
$k \sim \Delta\nu$

fast exchange
$k >> \Delta\nu$

- **Chemical or conformational exchange can be analyzed by NMR**
- **Rate constants can be determined, e.g. for a 2-state chemical reaction or conformational exchange:**

$$A \underset{k_{-1}}{\overset{k_1}{\rightleftharpoons}} B \qquad k_{ex} = k_1 + k_{-1}$$

NMR time scales

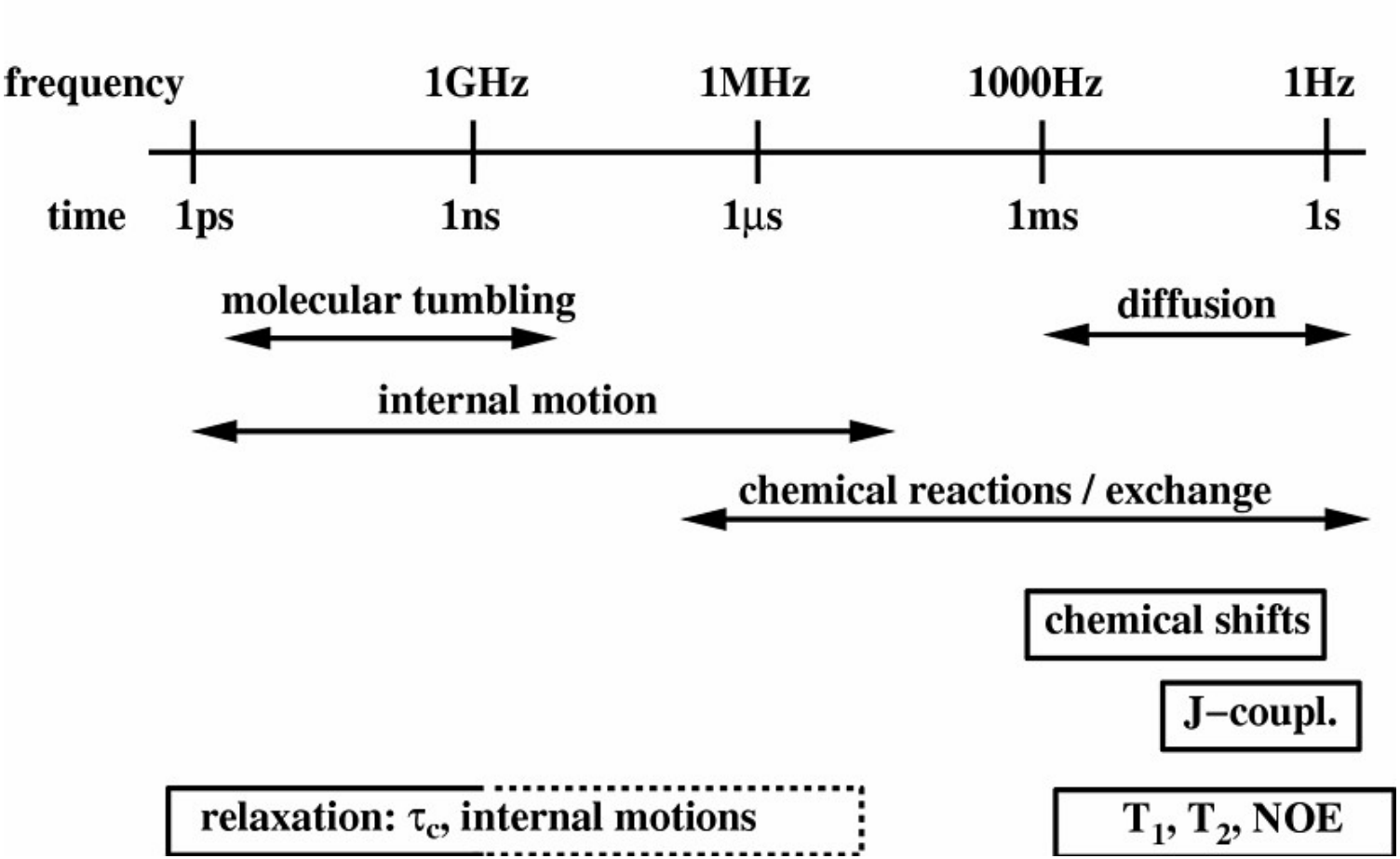

Residual Dipolar Couplings

Dipolar couplings are the physical basis for spin-spin cross-talk which causes relaxation and the NOE. The dipolar coupling between two spins depends on the internuclear distance *r* and its orientation with respect to the static magnetic field B_0.

$$D \sim 1/r^3 \langle 3\cos^2\theta - 1 \rangle$$

In the solid state, this leads to large dipolar splittings and huge linewidths since dipolar couplings, e.g. H-N are in the kHz range. In the liquid state, the orientation dependence and therefore D is averaged to zero.

If a molecule in solution is weakly aligned (10^{-3}) residual dipolar couplings (RDCs) can be reintroduced with a size of a few Hz. Thus, high-resolution spectra are obtained, but the distance and orientation dependence of D is reintroduced and provides valueable structural information.

For example, from the H-N dipolar couplings the projection angles θ and ϕ can be obtained.

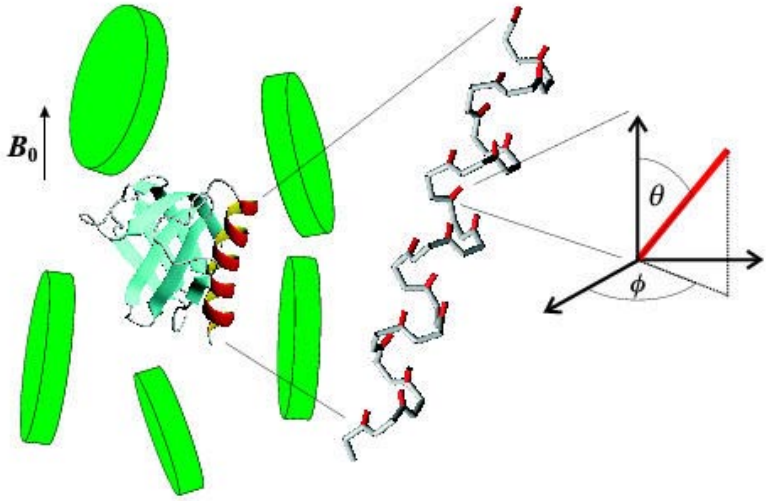

$$RDC = D_a \{(3\cos^2\theta - 1) + 3/2\ R \sin^2\theta \cos 2\phi\}$$

D_a and R describe the alignment tensor.
Biomolecules can be weakly aligned in dilute liquid crystalline media, e.g. bicelles (see figure).

NMR observables for structure and dynamics

Observable	Information
chemical shifts $^{1}H, ^{13}C, ^{15}N, ^{31}P$	**assignments,secondary structure**
J-couplings (through bond) $^{3}J(H^{N},H\alpha)$, $3J(H\alpha, H\beta)$, …	**dihedral angles: ϕ, χ, Karplus curves**
NOE (through space)	**interatomic distances (<5Å)**
solvent exchange (HN)	**hydrogen bonds**
relaxation / linewidths $^{1}H, ^{13}C, ^{15}N$	**mobility, dynamics** **conform./chem.exchange** **projection angles (ψ, …)**
residual dipolar couplings $^{1}H\text{-}^{15}N$, $^{1}H\text{-}^{13}C$, $^{13}C\text{-}^{13}C$, …	**projection angles**

Literature

NMR theory:

- Protein NMR spectroscopy – Principles and Practice.
  Cavanagh, Fairbrother, PalmerIII, Skelton. Academic Press (1996)

- Multidimensional NMR in liquids - Basic principles and experimental methods
  van de Ven, VCH (1995)

- Nuclear Magnetic Resonance Spectroscopy. Harris. Longman (1983)

- Principles of NMR in one and two dimensions. Ernst, Bodenhausen, Wokaun. Oxford (1989)

Biomolecular NMR:

- NMR of Proteins and Nucleic Acids. Wüthrich. Wiley (1986)

- Nature Struct. Biol. (1997) 4, 841-865 & 5, 492-522 (NMR supplement I & II)

- NMR spectroscopy of large molecules and multimolecular assemblies in solution.
  Wider, Wüthrich Curr. Op. Struct. Biol. (1999) 9, 594-601